Changes in aberrations and retinal image quality due to tear film dynamics

Kaccie Y. Li

The Institute of Optics and Center for Visual Science, University of Rochester, Rochester, NY 14627
yli@cvs.rochester.edu

Geunyoung Yoon

Department of Ophthalmology and Center for Visual Science, University of Rochester, Rochester, NY 14627
yoon@cvs.rochester.edu

Abstract: A reliable and objective method to measure aberration changes due to the tear film is essential in improving clinical assessment of the tear film and *in vivo* retinal imaging. The tear film of 11 subjects are studied by acquiring continuous wavefront measurements in real-time with a customized Shack-Hartmann wavefront sensor. The device has a high resolution lenslet array (190 μm) and a topographer unit with an infrared pupil illuminator (940 nm). A Fourier transform reconstructor algorithm [1] was used to estimate the eyes' wavefront aberrations from slope measurements. Increasing irregularities in the tear film produced observable wavefront variations. The temporal behavior of tear induced aberrations and retinal image quality was evaluated by the root mean squared (RMS) error of the residual wavefront and the volume modulation transfer function (MTF). Similar trends were observed from both metrics. Our analysis demonstrates the applicability of the SH wavefront sensor to assessing the dynamics of the human tear film.

OCIS codes: (330.5370) Physiological optics, (170.3890) Medical optics instrumentation, (330.4300) Noninvasive assessment of the visual system and (330.4460) ophthalmic optics.

References and Links

1. F. Roddier, and C. Roddier, "Wave-Front Reconstruction Using Iterative Fourier-Transforms," Appl. Opt. **30**, 1325-1327 (1991).
2. H. Hofer, P. Artal, B. Singer, J. L. Aragon, and D. R. Williams, "Dynamics of the eye's wave aberration," J. Opt. Soc. Am. A **18**, 497-506 (2001).
3. R. Montes-Mico, J. L. Alio, and W. N. Charman, "Dynamic changes in the tear film in dry eyes," Investigative Ophthalmology & Visual Science **46**, 1615-1619 (2005).
4. J. Craig, "Structure and function of the preocular tear film," in *The Tear Film: Structure, Function and Clinical Examination*, R. Edwards, and C. Hutchins, eds. (Butterworth-Heinemann, 2002), pp. 18-50.
5. R. Montes-Mico, J. L. Alio, G. Munoz, J. J. Perez-Santonja, and W. N. Charman, "Postblink changes in total and corneal ocular aberrations," Ophthalmology **111**, 758-767 (2004).
6. R. Tutt, A. Bradley, C. Begley, and L. N. Thibos, "Optical and visual impact of tear break-up in human eyes," Investigative Ophthalmology & Visual Science **41**, 4117-4123 (2000).
7. A. Dubra, C. Paterson, and C. Dainty, "Study of the tear topography dynamics using a lateral shearing interferometer," Opt.s Express **12**, 6278-6288 (2004).
8. S. Gruppetta, F. Lacombe, and P. Puget, "Study of the dynamic aberrations of the human tear film," Opt. Express **13**, 7631-7636 (2005).
9. D. R. Iskander, M. J. Collins, and B. Davis, "Evaluating tear film stability in the human eye with high-speed videokeratoscopy," IEEE Trans. Biomed. Eng. **52**, 1939-1949 (2005).
10. J. Nemeth, B. Erdelyi, B. Csakany, M. Gaspar, A. Soumelidis, F. Kablesz, and Z. Lang, "High-speed videotopographic measurement of tear film build-up time," Investigative Ophthalmology & Visual Science **43**, 1783-1790 (2002).
11. L. A. Carvalho, "Accuracy of Zernike polynomials in characterizing optical aberrations and the corneal surface of the eye," Investigative Ophthalmology & Visual Science **46**, 1915-1926 (2005).
12. M. K. Smolek, and S. D. Klyce, "Zernike polynomial fitting fails to represent all visually significant corneal aberrations," Investigative Ophthalmology & Visual Science **44**, 4676-4681 (2003).

#74914 - $15.00 USD Received 12 September 2006; accepted 9 October 2006

13. J. C. Wyant, and K. Creath, "Basic wavefront aberration theory for optical metrology," in *Applied Optics and Optical Engineering*, J. C. Wyant, and R. R. Shannon, eds. (Academic Press, 1992), pp. 2-53.
14. W. H. Southwell, "Wave-Front Estimation from Wave-Front Slope Measurements," J. Opt. Soc. Am. **70**, 998-1009 (1980).

1. Introduction

Understanding how the tear film affects the optical quality of the eye has both clinical and scientific importance. These may include improved diagnoses for tear film disorders and the capability of correcting the temporally fluctuating aberrations for retinal imaging with adaptive optics [2, 3]. The tear film, consisting of 90 percent aqueous material held in place by a 0.1 μm thick layer of lipid, forms the first surface of the eye where the change in the refractive index is the greatest [4]. As a result, the tear film is important for insuring the quality of the eye's optics and retinal image. Thus, it is generally believed to contribute the most to the observable changes in the eye's aberrations shortly after blink.

Our understanding of the tear film structure and its optical properties is still rather elementary. There is still no single test that can perform a complete evaluation of the tear film. The process of measuring aberrations induced by the tear film is difficult because many ocular aberrations are not only dynamic but highly irregular as well. As a result, many investigators have had limited success in quantifying these aberration changes using commercially available instruments [5, 6]. Some typical limitations imposed by commercial instruments include data acquisition speed, sampling resolution, and method of wavefront reconstruction. Nevertheless, there is sufficient evidence indicating that irregularities in the tear film structure that appears after an extended period of non-blinking can cause significant changes in the retinal image quality.

Only recently have we come to better understand the optical changes caused by the dynamic behavior of the tear film. The development of a shearing interferometer to observe the dynamics of the tear film topography by Dubra *et al.* [7] demonstrated a novel method for computing the RMS wavefront error from shearing interference fringes. Gruppetta *et al.* [8] took the curvature sensing approach that can map out the topography of the tear film at high speeds. Furthermore, improvements in data acquisition speed and eye-movement compensation for corneal topography have been made specifically to study the tear film as well [9, 10]. However, both these techniques are highly sensitive to eye movements making measurements reliable only over rather small pupils (3 and 4 mm diameters). The Shack-Hartmann (SH) wavefront sensor is refraction-based, so it is much less sensitive to eye movements. In addition, wavefront measurements can be usually made over pupils beyond 6 mm in diameter and can operate even faster than what has been reported in earlier studies. We implemented a high resolution SH sensor equipped with a custom-made corneal topographer and demonstrated its effectiveness in measuring the tear film induced aberrations changes in 11 subjects. Both the wavefront sensor and topographer is designed to use near infrared light illumination sources to avoid artificial stimulation of natural tear secretion process.

2. Method

2.1 Device specifications and experiment procedure

Figure 1 is a schematic diagram of the SH wavefront sensor developed for this study. The point source of light from the sensor is provided by a super luminescent diode (SLD) with a wavelength of 830 nm. The SLD beam is reflected onto the retina by a pellicle beam splitter (PBS). The backscattered light generates the aberrated wavefront at the pupil plane, which is than relayed onto the lenslets by a telescope with unit magnification. Light from the illuminator and SLD are separated into their corresponding paths by an appropriately specified dichroic mirror (DM). The lenslet array used has a resolution of 31 × 31, and each lenslet element is 190 μm in diameter and has a focal length of 10 mm. All measurements were made over a 6 mm diameter circular pupil with unit magnification. At this resolution, the

#74914 - $15.00 USD Received 12 September 2006; accepted 9 October 2006

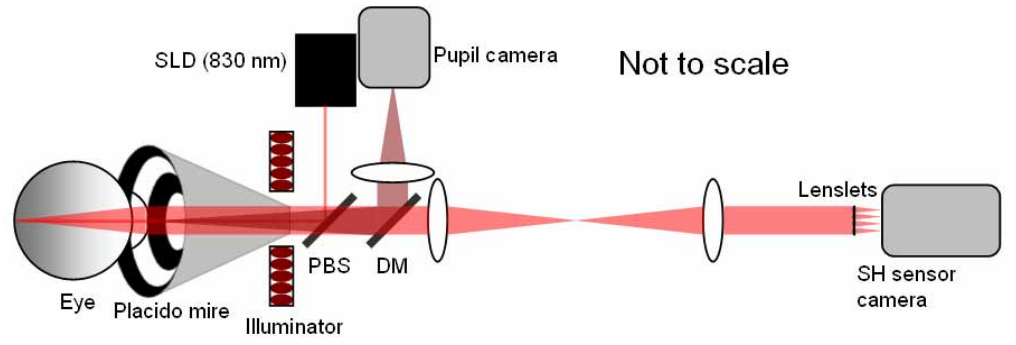

Fig. 1. Schematic diagram of the Shack-Hartmann wavefront sensor. The PBS places the beam from the SLD into the imaging path, and a dichroic mirror is used to separate the 940 nm light used to image the pupil and the aberrated wavefront at 830 nm.

wavefront slopes are sampled at 725 locations. The CCD camera used has a resolution of 1004 × 1004 pixels where the pixel size is 7.4 μm. A topographer unit is attached to the pupil camera for simultaneous observation of the tear film surface while making wavefront measurements. The placido mire is illuminated by an infrared (940 nm) ring illuminator as shown in Fig. 1. Infrared is used to avoid any effects of unnecessary visual stimuli for the subjects insuring the repeatability of the measurements. The pupil camera is placed conjugate to the lenslets to insure that the eye is placed at the right plane. With the added topographer, the black and white rings of the mire reflected off the cornea are captured by the pupil camera.

The eyes of 11 subjects were measured and recorded at 10 Hz. The experiment was done several times for each subject (40 measurements total), and each subject was given an hours rest between measurement sessions. Eight subjects had no tear film abnormalities, while the other 3 were diagnosed to have dry eye symptoms. Among the healthy subjects, 3 of them wore contact lenses regularly, but all measurements were made with their lenses removed. All subjects' eyes were dilated with 1 percent tropicamide, which also effectively removes any accommodation that can potentially introduce irrelevant aberrations into our measurements. Subjects are instructed to fixate on the SLD without blinking for as long as they voluntarily can (for up to 32 seconds). Image sequences from both cameras were recorded simultaneously in real-time and lasted from 3 to 32 seconds. A representative frame from both cameras is given in Fig. 2. The large range of measurement periods are simply due to the fact that healthy subjects can typically withstand much longer measurement sessions than those diagnosed with dry eyes.

2.2 Data analysis

All wavefront maps were generated using the Fourier transform reconstructor described by Roddier and Roddier [1]. The wavefront maps from the initial 5 frames (up to 0.5 seconds) were temporally averaged to define the eye's static aberrations, $W_{static}(x,y)$, for each measurement. We computed the residual wavefront map, $W_{Tear}(x,y,t)$, which is defined by

$$W_{Tear}(x,y,t) = W(x,y,t) - W_{static}(x,y) \quad (1)$$

where $W(x,y,t)$ is the wavefront at frame t, to represent the aberration changes induced by the tear film. Computing the residual wavefront map using modal reconstruction with Zernike polynomials is less accurate than the Fourier transform reconstructor for this application as illustrated in Fig. 3. Zernike modes up to 10^{th} order still fail to reconstruct several of the more abrupt changes in the residual wavefront. The zonal-based Fourier transform reconstructor [1] clearly provides a better representation of the aberrated wavefront as the tear film breaks up, so it was used to reconstruct $W(x,y,t)$. Via this reconstruction method the wavefront is

#74914 - $15.00 USD Received 12 September 2006; accepted 9 October 2006

computed locally across each lenslet, so the resolution of $W(x,y,t)$ is equal to that of the lenslet array.

The residual RMS wavefront error and the two-dimensional MTF calculated from the residual wavefront were used to evaluate the temporal behavior of the tear film induced changes in aberrations and retinal image quality. Both evaluation methods are included in the analysis for the purpose of assessing whether one form of quantification may be more appropriate than the other for this application. The volume MTF defined by

$$Volume(MTF,t) = \sum_{\omega \le 60 cpd} MTF(\omega,t) \tag{2}$$

is the retinal image quality metric used where ω is spatial frequency in cycles per degree (cpd). The highest detectable spatial frequency for human eyes is around 60 cpd, so the summation was defined over the circular band region up to that frequency. Temporal variability of both the residual RMS and the volume MTF is defined as the standard deviation about the temporal mean for each measurement session.

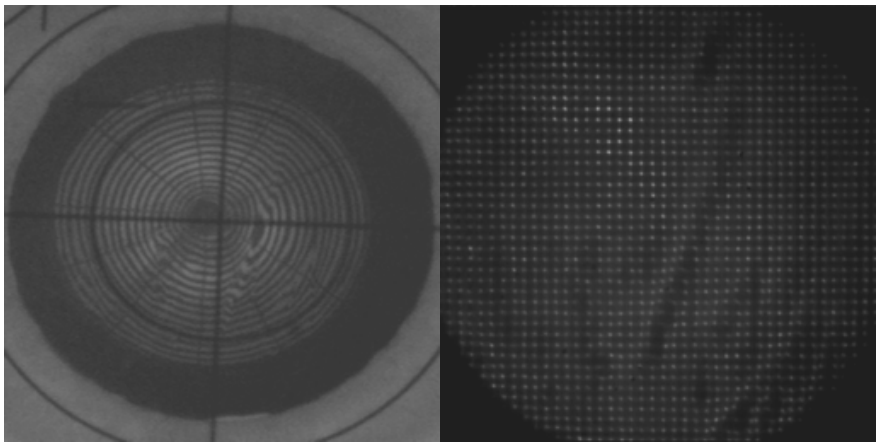

Fig. 2. Tear film breakup in a healthy eye due to a lengthy non-blink interval. Irregularities of the tear film surface are seen in both the reflection of the topography mires from the pupil cameral (a) and SH wavefront sensor image (b).

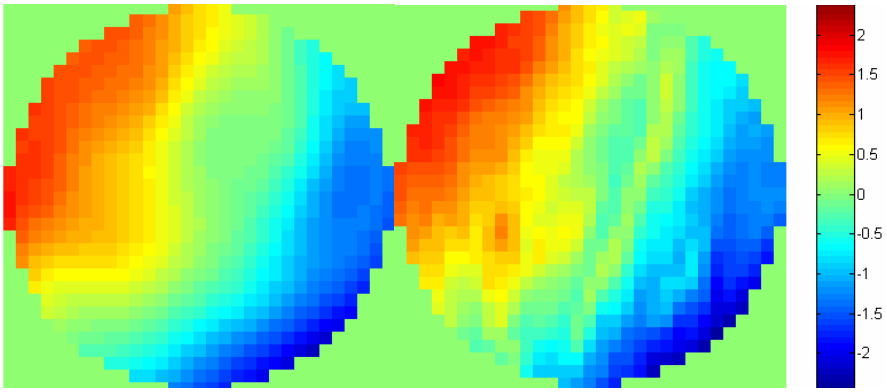

Fig. 3. Residual wavefront maps from the same SH data (shown in Fig. 2 above) using Zernike modes (a) and the Fourier transform reconstructor (b). Color bar is in microns.

#74914 - $15.00 USD Received 12 September 2006; accepted 9 October 2006

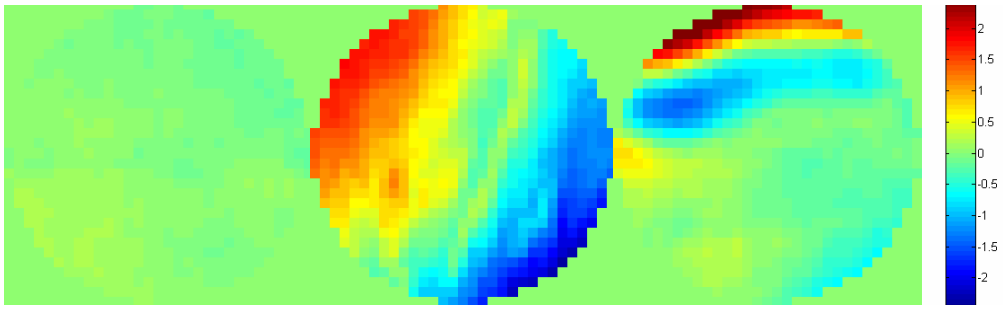

Fig 4. Movies illustrating the progression of the residual wavefront for a typical healthy eye with a highly stable tear film (a) (2.89 MB), the healthy eye corresponding to the raw data in Fig. 2 that has a less stable tear film (b) (2.54 MB) and a rather prominent dry eye (c) (3.12 MB). Color bar is in microns

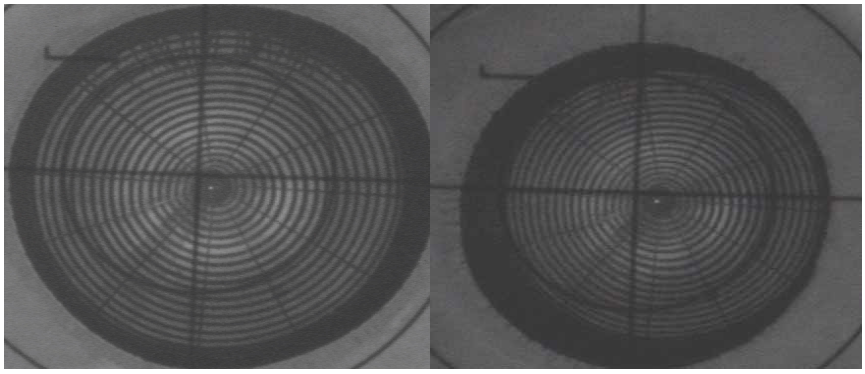

Fig. 5. Movies capturing the reflection of the topography mire on the pupil show the differences in tear film dynamics of a healthy eye (a) (3.42 MB) and a dry eye (b) (4.18 MB).

3. Results

The irregular "folds" and "ripples" in the tear film can be seen in both the topography and the HS sensor images as shown in Fig. 2. The tear film irregularities that may appear several seconds post-blink produces the spot displacements seen in the HS sensor image, and this information is used to reconstruct the residual wavefront as described by equation 1. Series of wavefront phase maps showing the dynamic aberration change due to the tear film from three different eyes are shown in Fig. 4. The residual wavefront for healthy eyes either show no spatial and temporal variability for the entire measurement session or modest degradations in comparison to dry eyes. An example of the residual wavefront map for each type of healthy eye is given in Fig. 4. More severe degradations were observed for dry eyes. Due to irritations that these subjects tend to experience over prolonged periods of non-blinking, measurement sessions tend to be considerably shorter (3 to 15 seconds). An example showing the residual wavefront fluctuations for a dry eye is given in Fig. 4(c). The wavefront map of a highly stable tear film does not, at any moment within the measurement session, deviate much from what it was immediately after blink. Unfortunately for dry eyes, the wavefront is only stable for the first several frames. Irregular fluctuations in the wavefront map quickly appear as the tear film surface degrades. This provides a more objective view of how dynamic behavior of the tear film correlate to fluctuations in the eye's aberrations.

Residual RMS steadily increased after blink as most eyes had observable degradations in the tear film within the measurement period. For healthy eyes whose tear films remained stable for the entire measurement session, modest fluctuations were observed from both the residual RMS and volume MTF. An example illustrating how tear film dynamics differed between healthy and dry eyes is shown by topography movies in Fig. 5. Both the residual

#74914 - $15.00 USD Received 12 September 2006; accepted 9 October 2006

RMS and volume MTF for these two measurements, shown in Fig. 6, clearly reflects the differences between the two eyes' tear film. As seen earlier in Fig. 2 and Fig. 4(a), occasionally the irregularities of the tear film can be seen in healthy eyes after extended non-blink intervals as well. Although highly observable at times, they do not produce the large monotonic variations in the residue RMS and volume MTF typically seen in measurements from dry eyes.

Figure 7 shows the evolution of the residual RMS and volume MTF from all successful measurements of the same dry eye and healthy eye represented in Figs. 5 and 6. Residual RMS remained stable for the healthy eye and increased in a highly variable manner between measurements immediately after blink for the dry eye. A similar trend can be observed from the corresponding plots of the volume MTF in Fig. 4(b). However, residual wavefront variability tend not as prominently reflected by the volume MTF as it was by the residual RMS. The mean temporal variability of both residual RMS and volume MTF were computed and reported in Table 1. Dry eyes showed more variability for the residual RMS and less variability for the volume MTF than healthy eyes even though data acquired from dry eyes generally represented much shorter time intervals.

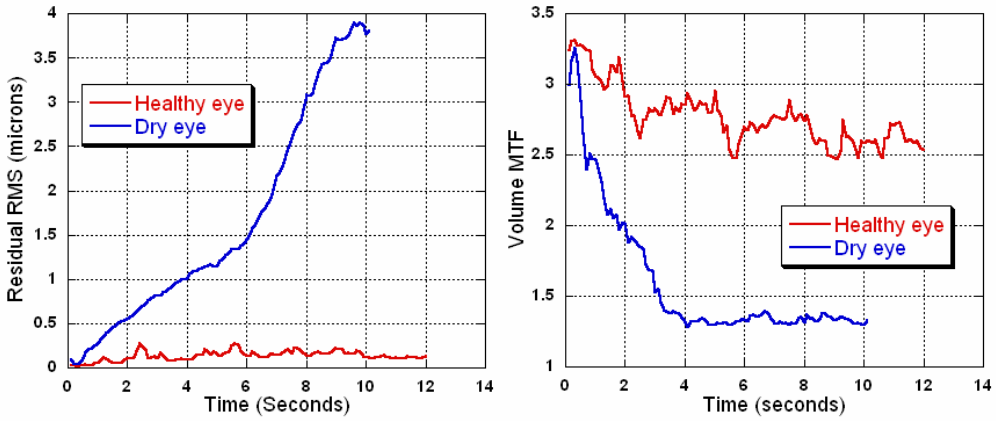

Fig. 6. Evolution of the residual RMS wavefront error (a) and volume MTF (b) for measurements corresponding to the movies in Fig. 5. Both evaluation metrics illustrates how the tear film of the healthy eye remained relatively stable in comparison with the dry eye

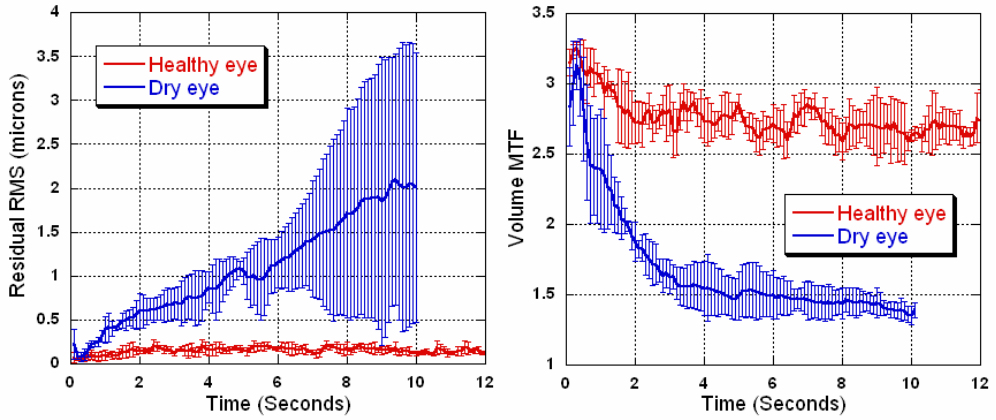

Fig. 7. Evolution of the residual RMS wavefront error (a) and volume MTF (b) from one healthy eye and one dry eye. Error bars represent standard deviations resulting from four separate measurements of the healthy eye and three of the dry eye. Data corresponds to the same pair of eyes represented in Figs. 5 and 6.

#74914 - $15.00 USD Received 12 September 2006; accepted 9 October 2006

Table 1. Temporal variability of residual RMS and volume MTF

Group	RMS (μm)	Volume MTF
Healthy	0.46 ± 0.49	0.66 ± 0.26
Healthy (CL)	0.55 ± 0.37	0.79 ± 0.20
Dry Eye	0.78 ± 0.63	0.75 ± 0.26

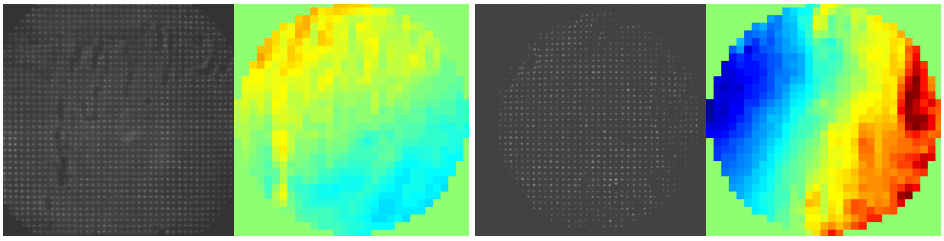

Fig. 8. A highly non-uniform optical surface due to the tear film produces more blurring and irregular spot displacements in the SH image. The corresponding aberrations induced by the tear film are clearly visible in the residual wavefront maps

4. Discussion

In wavefront sensing of the eye, modal reconstruction using Zernike polynomials has become the preferred method of wavefront estimation because certain Zernike modes are identical to several types of aberrations that appears naturally when considering optical image formation beyond the paraxial region. In most cases, a uniform layer of tear film covering the cornea can be represented accurately by a surface that consists of relatively lower spatial frequencies. As a result, the eye's optics primarily suffers from aberrations that can be accurately described by Zernike modes. The Fourier transform reconstructor is zonal-based, so it is naturally more sensitive to noise present in the SH sensor. For this reason, when only certain Zernike modes are present in the total wavefront, modal reconstruction via Zernike polynomials tends to be more accurate [14]. However when other higher order aberrations are introduced to the optical system, Zernike polynomials have been shown to perform poorly in many cases [11-13]. In this study, such aberrations are products of optical changes due to the tear film. In a similar study, Gruppetta *et al.* [8] reported that Zernike modes up to 9^{th} order still failed to fully represent the tear film features observed, which holds true, as shown in Fig. 3(b), for our measurements as well. Increasing the number of Zernike modes can add noise to the process and can potentially lower the accuracy of the result. Therefore in the presence of an irregular tear film, the Fourier transform reconstructor becomes the more appropriate solution as illustrated by the wavefront maps in Figs. 3 and 8.

Residual RMS and volume MTF were effective indicators of the increasing tear film irregularities. There does not seem to be any advantage in using one metric over the other. Our findings according to the residual RMS is comparable to what was reported in more recent studies [7, 8]. The actual values they reported were quite different from ours because their measurements were made over a much smaller pupil. Nevertheless, the behavior of how the residual RMS progressed after blink showed a similar trend. A comparison with results reported by Micos *et al.* [5] is more difficult because their calculations were based solely on data reconstructed via Zernike modes. Since it has already been shown in a previous study [8] and confirmed by this study that Zernike modes often fail to fully represent aberrations induced by the tear film, interpreting the data in this manner can potentially be misleading.

As for noninvasive clinical assessment of the tear film, the residual wavefront can provide sub-clinical information about the tear film condition that may not be as easily observable from tear surface topography alone. Furthermore, objective measurements in a noninvasive manner allow us to be more confident in our interpretation. Temporal variability in the

#74914 - $15.00 USD Received 12 September 2006; accepted 9 October 2006

residual RMS and volume MTF are generally higher for dry eyes due to the tendency for these participants to experience degradations in their tear film sooner and to a greater extent than those with healthy eyes. Statistical implications of this comparison have already been discussed in an earlier study [3], but the application of the SH sensor can be extended further clinically such as the assessment of different types of dry eyes.

5. Conclusion

Accurate measurements of aberration changes due to the tear film were made with a high resolution Shack-Hartmann wavefront sensor. This method of assessing the tear film and allows for faster acquisition speeds, and measurements can be made reliably over a larger pupil with better protection from eye movements. Zonal-based wavefront reconstruction via the Fourier transform reconstructor provided a more accurate representation of the irregular aberrations induced by a non-uniform tear film than reconstruction by Zernike decomposition.

Acknowledgments

This work was supported by grants from NIH (R01-EY014999), Rochester/Finger Lakes Eye and Tissue Bank and RPB. The authors would like to thank James Aquavella, Seth Pantanelli and Shan He for their assistance in the recruitment of research participants, development of the wavefront sensor and wavefront analysis software.

#74914 - $15.00 USD Received 12 September 2006; accepted 9 October 2006